Journal of Catalysis 320 (2014) 63–69

Contents lists available at ScienceDirect

Journal of Catalysis

journal homepage: www.elsevier.com/locate/jcat

# Chiral periodic mesoporous copper(II) bis(oxazoline) phenylene–silica: A highly efficient and reusable asymmetric heterogeneous catalyst

Mirtha A.O. Lourenço [a], Liliana Carneiro [b], Alvaro Mayoral [c], Isabel Diaz [d], Ana R. Silva [b,*], Paula Ferreira [a,*]

[a] *Department of Materials and Ceramics Engineering, CICECO, Universidade de Aveiro, 3810-193 Aveiro, Portugal*
[b] *Department of Chemistry, CICECO, Universidade de Aveiro, 3810-193 Aveiro, Portugal*
[c] *Laboratorio de Microscopias Avanzadas, Instituto de Nanociencia de Aragon, Universidad de Zaragoza, Edificio I+D, Mariano Esquillor, 50018 Zaragoza, Spain*
[d] *Instituto de Catálisis y Petroleoquímica, CSIC, c/Marie Curie 2, 28049 Madrid, Spain*

ARTICLE INFO

*Article history:*
Received 28 April 2014
Revised 23 August 2014
Accepted 22 September 2014
Available online 20 October 2014

*Keywords:*
Heterogeneous catalysis
Asymmetric catalysis
Homogeneous catalysis
Periodic mesoporous organosilicas
Co-condensation

ABSTRACT

We describe the preparation of an effective and reusable heterogeneous asymmetric catalyst. A novel chiral periodic mesoporous phenylene–silica containing high density of bis(oxazoline) moieties is prepared by co-condensation method with 1,4-bis(triethoxysilyl)benzene. After copper(II) coordination, the material is extremely efficient on the kinetic resolution of the 1,2-diphenylethane-1,2-diol with persistent high enantioselectivities (91 - > 99%) and yields (46–43% in maximum 50% resolution) at least for five consecutive cycles. Characterization of the material after the catalytic experiments showed that the heterogeneous catalyst was very robust keeping the integrity of the structure.

## 1. Introduction

Bis(oxazoline) are very versatile chiral ligands in asymmetric catalysis (Scheme 1) and a large number of organic transformations have been enantioselectively catalyzed by their transition metal complexes [1]. These ligands are commercially available, but are expensive. Therefore there has been an intense research effort in order to make them recyclable and reusable, thus economical [2–6]. The most successful strategy has been the covalent immobilization onto several supports [2–5]. Asymmetric heterogeneous catalysts obtained using some organic polymers [7,8] or siliceous mesocellular foams [9,10] as supports have been superior to those using copper(II) bis(oxazoline) post-grafted onto ordered mesoporous silicas [11–13] or mesoporous carbons [12,13]. The enantioselectivity was influenced by the active phase density [6,12–14] and the capping of the siliceous mesocellular foam silanols [9,10,14].

The design of periodic mesoporous organosilicas (PMOs) containing catalytic active sites as part of the material framework is a relatively new strategy for the preparation of heterogeneous catalysts based on versatile and successful homogeneous catalysts [15–23]. These materials show high density of active sites on the pore surfaces [17] and high recyclability [15]. The well dispersed catalytic sites partially integrated on the wall of these materials offer reduced resistance to the diffusion of molecules within the mesochannels and are more resistant to leaching than if they were grafted onto the ordered mesoporous silica [17].

The synthesis of PMOs incorporating chiral privileged ligands is still quite un-explored and the synthesis of chiral PMOs with high catalytic activity and enantioselectivity remains a challenge, especially in the case of bis(oxazoline) ligands [22,23].

Hence, here we describe the synthesis and characterization of a novel periodic mesoporous organosilica bearing a high density of chiral bis(oxazoline) ligands by co-condensation of 1,4-bis(triethoxysilyl)benzene (BTEB) with trimethoxypropylsilane difunctionalized commercial bis(oxazoline) [13,24] (Scheme 2) in the presence of a surfactant. After coordination of [Cu(OTf)$_2$], this material acts as a very efficient asymmetric heterogeneous catalyst in the kinetic resolution of the 1,2-diphenylethane-1,2-diol with high enantioselectivity and yield, keeping such high performance for at least five consecutive cycles.

## 2. Experimental

### 2.1. Chemicals and reagents

Copper(II) trifluoromethanosulfonate (copper(II) triflate, [Cu(OTf)$_2$], 98%), 2,2′-methylenebis[(4*S*)-4-phenyl-2-oxazoline]

---

* Corresponding authors at: Departamento de Química, CICECO, Universidade de Aveiro, Campus Universitário de Santiago, 3810-193 Aveiro, Portugal. Fax: +351 234 401 470 (A.R. Silva). Department of Materials and Ceramics Engineering, CICECO, Universidade de Aveiro, 3810-193 Aveiro, Portugal (P. Ferreira).

*E-mail address:* ana.rosa.silva@ua.pt (A.R. Silva).

http://dx.doi.org/10.1016/j.jcat.2014.09.017
0021-9517/

(**1**, 97%), (*S*)-(−)-2,2'-isopropylidenebis(4-phenyl-2-oxazoline) (**2,** 97%), butyl lithium solution 1.6 M in hexane, 3-iodopropyltrimethoxysilane (IPS, ⩾95.0%), triethylamine (Et$_3$N, ⩾99%), dry tetrahydrofuran (THF, ⩾99.9%), (*R*,*R*)-1,2-diphenyl-1,2-ethanediol (99%), (*S*,*S*)-1,2-diphenyl-1,2-ethanediol (99%), *N*,*N*-diisopropylethylamine (DIPEA, 99%), benzoyl chloride (99%), potassium hydroxide (p.a.) and potassium bromide (FT-IR grade, ⩾99%) were purchased from Aldrich and used as received. Ethanol (p.a.) and methanol (p.a.) were from Riedel de Häen. Dichloromethane, *n*-hexane, isopropanol and ethyl acetate were from Romil and HPLC grade. The octadecyltrimethylammonium bromide surfactant template (ODTMABr, 98%) was obtained from Aldrich.

### 2.2. Synthesis of the 1-Ph-PMO material

This method has three main steps: (i) functionalization of ligand **1** [13], (ii) hydrolysis and co-condensation of functionalized **1** with 1,4-*bis*(triethoxysilyl)benzene (BTEB) [25] and (iii) extraction of the octadecyltrimethylammonium bromide (OCTMABr) template. First, 0.60 mmol of **1** were reacted with 1.49 mmol of butyl lithium (1.6 M in hexane, BuLi) in 10 ml of dry tetrahydrofuran, under inert atmosphere. Then this solution was cooled with liquid nitrogen and 1.97 mmol of 3-iodopropyltrimethoxysilane were added drop-wise during 30 min. After stirring for 3 days at room temperature, under inert atmosphere, the color changed to red-brown [13]. Secondly, the synthesis of 1-Ph-PMO was performed using a mixture with molar ratios BTEB: functionalized **1:** ODTMABr: NaOH: H$_2$O: THF of 1: 0.23: 1.15: 5.07: 647: 7.44. In a typical synthesis the ODTMABr was dissolved in a mixture of ultrapure water and 6 M aqueous sodium hydroxide at 20–60 °C. The precursors mixture (functionalized **1** and BTEB) previously dissolved in THF, was subsequently added drop-wise under vigorous stirring, at room temperature. This solution was kept for 10 min in an ultrasonic vessel and stirred for 24 h at room temperature. After 24 h ageing in a Teflon flask at 100 °C, the resultant precipitate was recovered by filtration and dried at 60 °C. Finally, the surfactant was removed through solvent extraction. 0.5 g as-synthesized sample was stirred in 125 mL ethanol, for 12 h at 90 °C. The powder was filtered, washed with ethanol and water and dried overnight at 60 °C.

### 2.3. Preparation of the Cu@1-Ph-PMO material

To 0.24 g of the 1-Ph-PMO material a solution of 0.21 mmol of copper(II) triflate in 40 mL of methanol were added. After refluxing the mixture for 24 h, the solid was isolated by filtration, washed with methanol and dried under vacuum at 60 °C for 6 h. A light green material was obtained.

### 2.4. Preparation of the graf_Cu-1@Ph-PMO material (post-grafting)

The phenylene PMO (Ph-PMO) was synthetized following the literature procedures [26] by hydrolysis and condensation of BTEB in the presence of an ODTMABr surfactant. The template extraction was made using an ethanol–HCl solution. The Ph-PMO (0.37 g) was dried at 120 °C under vacuum atmosphere during 3 h to activate the pores. Then 10 mL of dry dichloromethane containing 0.089 mmol of dissolved copper(II) functionalized **1** (see 2.i) and 0.3 mL of triethylamine were dropped [13]. The mixture was refluxed, under inert atmosphere, for 6 h followed by stirring at room temperature for 48 h. The obtained material was filtered, washed successively 2 × 20 mL of THF, 2 × 20 mL of CH$_2$Cl$_2$, 2 × 20 mL of MeOH, refluxed with 20 mL of THF for 6 h, under inert atmosphere, and stirred at room temperature for 24 h. After filtration, the material was dried in an oven at 60 °C overnight.

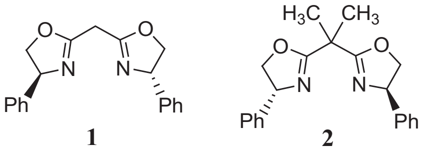

**1** **2**

**Scheme 1.** Chiral bis(oxazoline) ligands.

### 2.5. Physical and chemical methods

Elemental analysis was performed in triplicate by "Servicio de Análisis Instrumental", CACTI Vigo, Universidade de Vigo, Spain. The copper ICP-AES was performed at "Laboratório Central de Análises" of the University of Aveiro, Portugal. FTIR spectra were collected in the range 400–4000 cm$^{-1}$ at room temperature using a resolution of 4 cm$^{-1}$ and 256 scans by attenuated total reflectance (ATR) using a Bruker Tensor 27 spectrophotometer; the samples were dried in an oven at 100 °C for 12 h prior to the analysis. Thermogravimetry analyses (TGA) were performed under air flux with a ramp of 5 °C/min in a TGA apparatus, model Shimadzu TGA-50. Nitrogen adsorption isotherms at −196 °C were measured in an automatic apparatus (Gemini V 2.00 instrument model 2380; Micromeritics). Before the adsorption experiments the samples were outgassed under vacuum overnight at 150 °C (to minimize destruction of functionalities) to an ultimate pressure of 1024 mbar and then cooled to room temperature. The specific surface areas ($S_{\mathrm{BET}}$) were determined by the BET method. The pore size distributions (PSD, the differential volume adsorbed with respect to the differential pore size per unit mass as a function of pore width) were calculated by the BJH method using the modified Kelvin equation, using the adsorption branch of the experimental data [27]. The adsorption branch was used as it is known to be more accurate specially if the typical hysteresis of the mesoporous materials is of H2 type. In this case, the pore size distribution obtained from the desorption branch of the isotherm noticeably deviates from that of the adsorption branch and gives an incorrect pore size distribution [28]. X-band electron paramagnetic resonance (EPR) was performed at RIAIDT, Universidade de Santiago de Compostela, Spain, with frequency of 9.434 GHz and 100 kHz field modulation at 120.5 K. The reported EPR parameters were obtained by simulation using the program Win EPR Simfonia (Bruker) assuming axial spin Hamiltonians. The values of $g_{\perp}$ and $A_{\perp}$ are less accurate because of their dependence on the line widths (∼100 G) used in the simulations.

Powder X-ray diffraction (PXRD) data were collected with a Phillips X'Pert MPD diffractometer using Cu K$\alpha$ radiation. $^{13}$C, $^{29}$Si and spectra were recorded on a Bruker Avance III 400 spectrometer operating at 9.4 T. $^{13}$C cross-polarization magic-angle spinning (CP MAS) NMR spectra were recorded with 4 μs $^{1}$H 90° pulse, a contact time (CT) of 1 ms, a spinning rate ($\nu_R$) of 8 kHz and recycle delay (RD) of 4 s. $^{29}$Si MAS NMR spectra were collected employing a 40° flip angle pulse, a $\nu_R$ of 5 kHz and RD of 60 s. $^{29}$Si CP MAS NMR spectra were acquired with a 4 μs $^{1}$H 90° pulse, a CT of 8 ms, a $\nu_R$ of 5 kHz and RD of 5 s. The $^{13}$C and $^{29}$Si NMR spectra were quoted in ppm from trimethylsilane. The samples for transmission electron microscopy (TEM) analysis were finely crushed with mortar and pestle and dispersed in ethanol. C$_s$-corrected STEM-HAADF observations were carried out in a FEI Titan X-FEG 300-60, operated at 80 kV, equipped with a CEOS spherical aberration corrector for the electron probe, an EDAX EDS detector and a Gatan Tridiem Energy Filter for spectroscopy measurements.

### 2.6. Catalysis experiments

All the catalytic reactions of the prepared materials were performed in batch reactors at atmospheric pressure and with constant stirring. The kinetic resolution of 1,2-diphenylethane-1,2-diol (**3**)

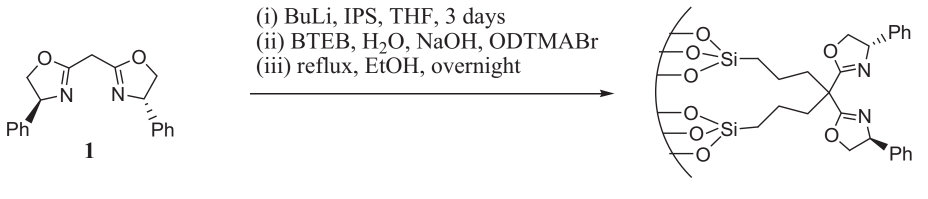

**1-Ph-PMO**

**Scheme 2.** Synthesis of the periodic mesoporous organosilica 1-Ph-PMO.

was performed at 0 °C using 0.48 mmol (*R*,*R*)-1,2-diphenylethane-1,2-diol, 0.48 mmol (*S*,*S*)-1,2-diphenylethane-1,2-diol, 1.00 mmol DIPEA (170 µl), amount of heterogeneous catalyst containing 1.0% mol Cu and 0.50 mmol of benzoyl chloride (58 µl) in 5.00 ml of dichloromethane [13,29]. The mixture was stirred for 24 h and after filtration of the heterogeneous catalyst the solvent was evaporated from the filtrate and the monobenzoylated product (**4**, Scheme 3) isolated by column chromatography over silica gel using *n*-hexane/ethyl acetate 3:1 as eluent. The **4** enantiomeric excess was determined by HPLC at 254 nm using a Chiralcel OD column (250 mm × 4.6 ID, 5 µm) and *n*-hexane/isopropanol 9:1 as eluent. The retention times of the (*R*)-**4** and (*S*)-**4** enantiomers were identified by comparison with those of a racemic **4** (see Figs. S1 and S2, SD). The reaction selectivity (*S*) was calculated based on the isolated yields of **4** and respective enantiomeric excess by using the formulae: $\ln[1 - \text{yield}(1 + ee)]/\ln[1 - \text{yield}\,(1 - ee)]$. The isolated materials at the end of the reactions were washed extensively with the appropriate solvent, dried under vacuum and reused in another cycle using the same experimental procedure. Control experiments were also performed using the same experimental procedure in homogeneous phase with equimolar quantities of $[Cu(OTf)_2]$ plus **1** or **2** in order to compare with the heterogeneous ones.

## 3. Results and discussion

Initially, the commercial bis(oxazoline) ligand **1** (Scheme 1) was functionalized with two trimethoxypropylsilane groups (Scheme 2), using a reported procedure [13,24]. The 1-Ph-PMO (Scheme 2) was synthesized following a typical co-condensation synthesis [30] with minor modifications in the presence of octadecyltrimethylammonium bromide (ODTMABr), which was extracted at the end of the reaction.

Elemental analysis of 1-Ph-PMO shows that the material has nitrogen, probing the presence of the bis(oxazoline) ligand **1**. Taking into consideration that each **1** ligand contains two atoms of nitrogen, a loading of 816 µmol/g can be calculated (Table 1). This value is much higher than the amount of **l** post-grafted onto other ordered mesoporous silicas such as SBA-15 [13]. Hence the **1** density in the 1-Ph-PMO is 1.1 $\mu mol/m^2$, whereas 0.4–0.05 $\mu mol/m^2$ were reached by post-grafting trimethoxypropylsilane functionalized **1** onto conventional ordered mesoporous silicas [13]. After coordination of $[Cu(OTf)_2]$ complex, a copper loading of 120 µmol/g onto the 1-Ph-PMO (Cu@1-Ph-PMO) was obtained by ICP-AES, yielding an excess of **1** to copper essential to the catalytic asymmetric process (Table 1). For comparison, a similar material was prepared via secondary grafting, i.e. the trimethoxypropylsilane functionalized copper(II) bis(oxazoline) onto [13] the phenylene PMO. Herein, the grafted material is denoted graf_Cu-1@Ph-PMO. In this material the ligand and the copper loadings were calculated to be 96 and 57 µmol/g (Table 1), respectively, which are much lower values than for Cu@1-Ph-PMO.

Due to the high **1** ligand content, the characteristic C = N stretching vibration can be clearly seen at 1649 $cm^{-1}$ in the ATR–FTIR spectrum of the novel 1-Ph-PMO (Fig. 1), besides of other characteristic vibrations at 3065 $cm^{-1}$ (Fig. S3, SD), between 1500–1400 and 800–700 $cm^{-1}$. The C=N stretching vibration is shifted to lower energy when compared with the free **1** ligand. New very strong Si–O stretching vibrations of the organosilica framework can now be also observed around 1043 $cm^{-1}$ in the 1-Ph-PMO spectrum. It is noteworthy that the presence of isolated silanols cannot be distinguished at 3750 $cm^{-1}$ (Fig. S3, SD). The ATR–FTIR spectrum of the Cu@1-Ph-PMO is very similar to that of 1-Ph-PMO, but the presence of S=O stretching vibrations from the sulfonate group of the triflate anion can be detected at 638 $cm^{-1}$.

The X-band EPR spectrum of the Cu@1-Ph-PMO material was taken at 120.5 K in the solid state and is depicted in Supplementary Data (Fig. S4, SD), together with the simulated spectra. It shows a signal typical of magnetically diluted copper species where the hyperfine structure from the coupling of the free electron with the Cu(II) nucleus ($I = 3/2$) can be clearly seen. The spectrum is axial with $g_{||}$ and $g_{\perp}$ of 2.265 and 2.075, respectively, and $A_{||} = 182 \times 10^{-4}$ $cm^{-1}$ obtained by simulation of the spectra (Fig. S4, SD). When compared to the reported parameters for $[Cu(OTf)_2]$ in frozen solution ($g_{||} = 2.412$, $g_{\perp} = 2.083$ and $A_{||} = 134.5 \times 10^{-4}$ $cm^{-1}$), the g values are lower and the higher $A_{||}$ indicates that there are nitrogen atoms in the coordination sphere. The simulated parameters are also close to the ones reported for

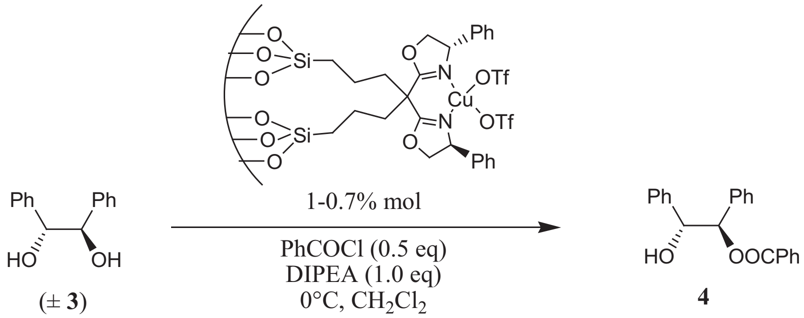

**Scheme 3.** Kinetic resolution of 1,2-diphenylethane-1,2-diol (**3**) by Cu@1-Ph-PMO.

**Table 1**
Chemical and textural characteristics of the PMO materials.

| Sample | Concentration (μmol/g) | | [Ligand]/[Cu] | Textural properties | | Density (μmol/m$^2$) | |
|---|---|---|---|---|---|---|---|
| | Cu[a] | Ligand[b] | | $A_{BET}$ (m$^2$/g) | $A_{ext}$ (m$^2$/g) | Cu | Ligand |
| 1-Ph-PMO | | 816 | | 637 | 1033 | | 1.3 |
| Cu@1-Ph-PMO | 120 | 740 | 6.2 | 684 | 1049 | 0.2 | 1.1 |
| graf_Cu-1@Ph-PMO | 57 | 96 | 1.7 | 664 | 834 | 0.1 | 0.2 |

[a] Determined by ICP-AES.
[b] Determined by EA from the nitrogen content.

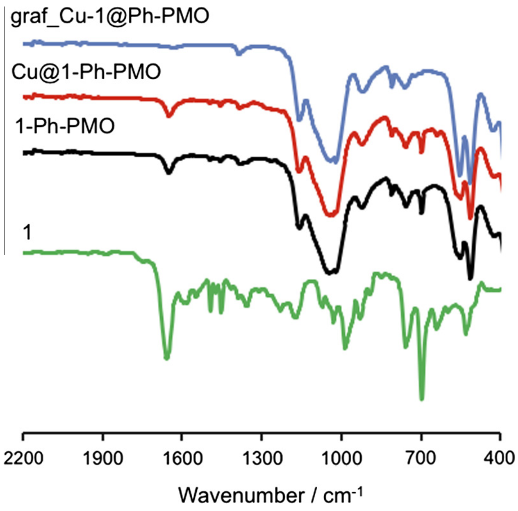

**Fig. 1.** ATR–FTIR spectra of the 1, 1-Ph-PMO, Cu@1-Ph-PMO and graf_Cu-1@Ph-PMO.

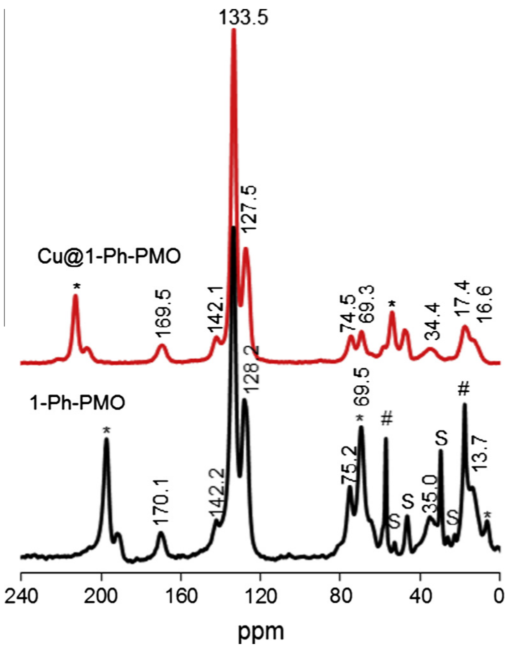

**Fig. 2.** $^{13}$C CP-MAS NMR spectra of 1-Ph-PMO and Cu@1-Ph-PMO. Asterisks depict spinning side bands. Cardinals represent ethanol impurities. S is used to identify the surfactant residual peaks.

the Cu-**1** complex in frozen solution indicating that Cu(II) coordination to the bis(oxazoline) nitrogen atoms took place (Scheme 2) [31].

Solid-state $^{13}$C CP MAS NMR spectra of 1-Ph-PMO and Cu@1-Ph-PMO materials are shown in Fig. 2. The 1-Ph-PMO spectrum shows resonances between 9 and 20 ppm that can be assigned to the $CH_2$ carbons of the propylsilane ligands. The peak at 35.0 ppm corresponds to the quaternary carbon that binds the two oxazoline rings to the propylsilane ligands. The two peaks at 69.5 and 75.2 ppm are related with the *sp*$^3$ carbons of the oxazoline rings, linked to, respectively, the N and the O atoms. In the same spectrum it is possible to observe resonances at 128.2, 133.5 and 142.2 ppm assigned to the *sp*$^2$ carbons from the phenyl groups. The peak at 142.2 ppm should correspond to the *sp*$^2$ carbons of the phenyl rings directly bounded to the oxazolines. The peak at 133.5 ppm is assigned to the *sp*$^2$ carbons of the phenylene bridge from the BTEB precursor. Finally, the peak at 170.1 ppm is attributed to the *sp*$^2$ carbons directly linked to both N and O atoms of the oxazolines. Other small peaks in the spectrum between 10 and 75 ppm may correspond to residual carbons of the alkyl chain of the surfactant. The $^{13}$C CP MAS NMR spectrum of Cu@1-Ph-PMO is very similar to the spectrum of 1-Ph-PMO but it seems slightly cleaner probably because the copper coordination is carried out in methanol at 80 °C, allowing a complete surfactant removal. The similar spectrum results from the non-coordinated bis(oxazoline) ligands. As Cu(II) is a paramagnetic nucleus it precluded the observation of the carbon nuclei close to it and only the non-coordinated can be observed.

The $^{29}$Si MAS and CP MAS NMR spectra of 1-Ph-PMO and Cu@1-Ph-PMO are shown in Fig. S5 of SD. An overlapping of the *T* environments [$T^m = RSi(OSi)_m(OH)_{3-m}$] resulting from the condensation of the BTEB and trimethoxypropylsilane functionalized **1** is observed. The 1-Ph-PMO spectrum shows three intense peaks at *ca.* −62, −71 and −81 ppm assigned to $T^1$, $T^2$ and $T^3$ organosiliceous species of BTEB. The *T* environments of the **1** ligand are less intense and seem to be slightly shifted to low field under the signals of the BTEB.

The structural order before and after copper coordination was evaluated by powder X-ray diffraction (PXRD) and transmission electron microscopy (TEM). PXRD pattern of 1-Ph-PMO (Fig. 3) reveals the characteristic low angle diffraction peaks at $d = 4.50$ nm ($2\theta = 1.96°$) usually associated with mesoporous materials. In addition a medium-range reflection is observed at $d = 0.764$ nm ($2\theta = 11.58°$) due to the molecular-scale periodicity along the wall.

In this way the 1-Ph-PMO material displays both meso- and molecular-scale periodicities. Upon copper coordination and after use of Cu@1-Ph-PMO as catalyst, the materials seem to preserve the structure (Fig. 3). The Cu@1-Ph-PMO before and after catalysis present a first low angle reflection at $d_{100} = 4.46$ and 4.41 nm, respectively (Table S1, SD). At a medium scattering angle, these two materials display peaks at $d = 0.765$ ($2\theta = 11.57°$) and 0.762 nm ($2\theta = 11.61°$), respectively (Fig. 3).

The presence of mesopores in the novel 1-Ph-PMO, Cu@1-Ph-PMO and graf_Cu-1@Ph-PMO is also supported by the nitrogen adsorption–desorption isotherms collected at −196 °C (see SD, Fig. S6). Type IV $N_2$ adsorption–desorption isotherms characteristic of mesoporous materials were observed together with narrow pore size distribution (PSD). The BET specific surface area of 637 m$^2$ g$^{-1}$

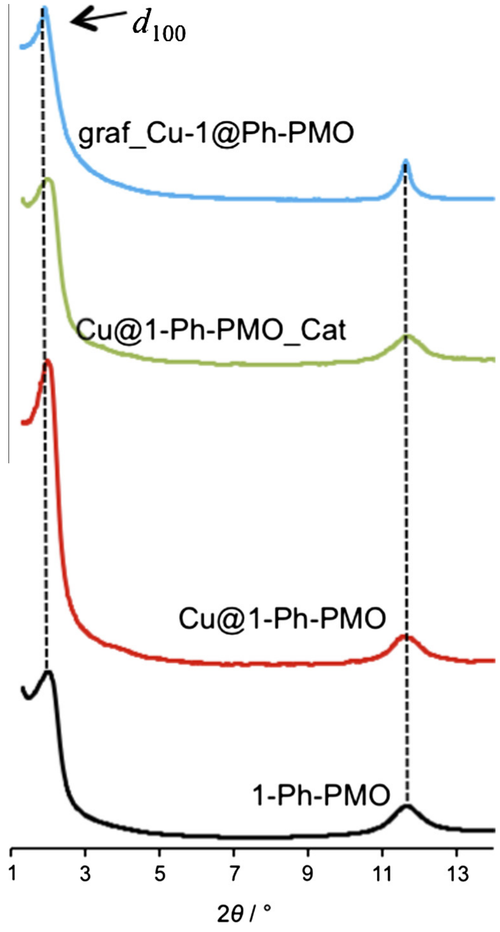

**Fig. 3.** XRD patterns of 1-Ph-PMO, Cu@1-Ph-PMO before and after catalysis, and graf_Cu-1@Ph-PMO.

(Table 1) obtained for the 1-Ph-PMO is much higher than a previous attempt to synthesize a hybrid organic–inorganic material by co-condensation of tetraethoxysilane (TEOS), instead of BTEB, with silane-functionalized bis(oxazoline) ligands.[32] The coordination of [Cu(OTf)$_2$] complex leads to an increase of the BET specific surface area to 684 m$^2$ g$^{-1}$, supporting the $^{13}$C CP MAS NMR evidence that the use of methanol as solvent helps to clean the material from surfactant residues.

Spherical aberration (C$_s$) corrected scanning transmission electron microscopy (STEM) observations were performed at 80 kV due to the beam sensitivity of C-containing mesoporous materials under the electron beam. The STEM-HAADF mode was chosen in an attempt to distinguish the pending groups with metal atoms using *Z* contrast. However, the observations did not yield enough evidences and therefore EDS was employed systematically to probe the presence of Cu and to corroborate a homogeneous distribution throughout the Cu@1-Ph-PMO material (see Fig. S7, SD). Fig. 4a shows the morphology of the 1-Ph-PMO with the pore system perpendicular to the electron beam. Cu@1-Ph-PMO is presented in Fig. 4b again along the [110] orientation. In the inset, the microstructure of the walls can be easily observed with a spacing of *d* = 0.795 nm (top left) and the pore openings (bottom left).

Nevertheless, using EELS nitrogen can also be detected in the 1-Ph-PMO material corroborating the elemental analysis (Fig. S8, SD). It is possible to confirm based on the TEM micrographs (Fig. 4) that the 1-Ph-PMO and Cu@1-Ph-PMO materials are mainly long range disordered, displaying only local hexagonal arrangement of pores (Fig. 4b – inset), corroborating the lack (or low intensity) of the (110) and (200) peaks characteristics of a two-dimensional hexagonal symmetry (p6 mm) lattice in the XRD patterns (Fig. 3). The pore size calculated from the TEM image is approximately 3 nm, which is in good agreement with the pore size obtained from the N$_2$ sorption isotherms (3 nm). Fig. S9 (SD) displays the micrograph images in which the ordered microstructure of the walls is evident. A low atomic percentage (below 1%) of Cu was verified by EDS measurement (Fig. S10).

The thermogravimetric analyses of 1-Ph-PMO and Cu@1-Ph-PMO (Fig. S11, SD) exhibit a first weight loss below 100 °C due to desorption of physisorbed water. The 1-Ph-PMO material has a thermal stability up to 200 °C. Above this value, the decomposition and release of the **1** organic bridges from the framework takes place. Above 500 °C, occurs the decomposition of the phenylene organic moieties. In the case of the Cu@1-Ph-PMO material, the decomposition of the **1** occurs at the same range of temperature, followed by the degradation of the triflate anion. CuO should be formed which may catalyze the combustion of the phenylene organic moieties at a lower temperature than in the copper free 1-Ph-PMO material (starts to occur at *ca.* 450 °C).

Copper(II) complexes with ligand **2** act as efficient homogeneous catalysts in the kinetic resolution of 1,2-diols [29]. Hence, we decided to test the Cu@1-Ph-PMO material as a heterogeneous catalyst in the asymmetric benzoylation of hydrobenzoin (Scheme 3). The results are compiled in Table 2, together with control experiments without the addition of catalyst and in homogeneous phase using ligand **1** and **2**. It can be concluded that the Cu@1-Ph-PMO material acts as a very efficient heterogeneous catalyst with high enantioselectivity and yield, using only 1% mol of Cu. Furthermore, the high enantioselectivities (91 – >99%) and yields (46–43% in maximum 50% resolution) could be sustained upon five consecutive reuses with 1–0.7% mol based on Cu. The enantioselectivities are also higher than the Cu(II) complex with the starting commercial bis(oxazoline) **1**, in 1% mol and similar to that of the methylated bis(oxazoline) **2** (Scheme 1). Thus propylation of the carbon bridge yields a more enantioselective heterogeneous catalyst than the corresponding homogeneous catalyst. These results are comparable to the reported heterogeneous catalysts based on the Cu(II) aza-bis(oxazoline) supported onto poly(ethyleneglycol) [33] and magnetic nanoparticles coated with silica [34] and carbon [35]. Post-grafting the Cu(II) complex with trimethoxypropylsilane functionalized **1** onto periodic mesoporous phenylenesilica resulted in lower catalyst density at the surface of the material and thus in a less efficient heterogeneous catalyst with significantly lower selectivity, enantioselectivity and yield. The high bis(oxazoline) density seems to be an important factor when compared with similar catalysts in the literature [13].

At the end of the five consecutive cycles the Cu@1-Ph-PMO material was also characterized by ATR–FTIR (SD, Fig. S12) and XRD (Fig. 3). Both techniques showed that there were not significant differences between the original Cu@1-Ph-PMO and after the catalytic cycles, confirming the chemical and structural integrity of the mesoporous material (Table S1, SD), respectively, and that it acts as a reusable asymmetric heterogeneous catalyst.

The higher metal density, catalytic activity and stability of the Cu@1-Ph-PMO in comparison to the graf_Cu-1@Ph-PMO may result from the co-condensation methodology of synthesis. As it was observed recently in SBA-15 [36], the introduction of the organic ligands during the formation of the mesoporous structure originate homogeneous materials with local geometries and environments that are prone to metal bind, creating stable catalytic sites comparable to the ones present in homogeneous catalysts.

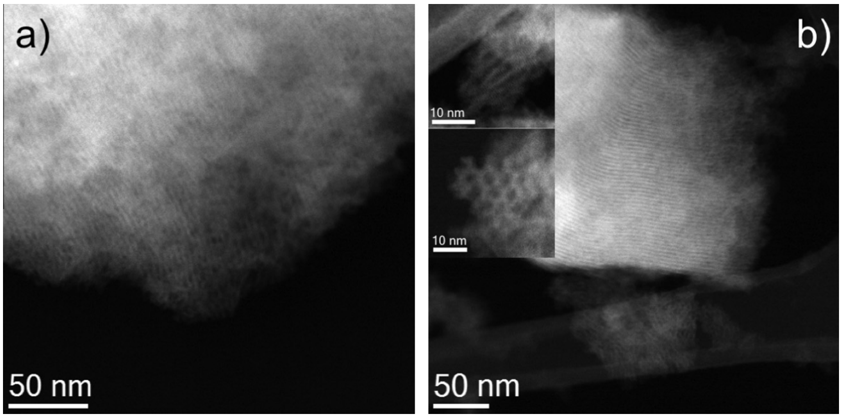

**Fig. 4.** $C_s$-STEM-HAADF micrograph images of (a) 1-Ph-PMO and (b) Cu@1-Ph-PMO. The top left inset represents the wall microstructure, while the bottom left shows the top view of the hexagonal arrangement of pores.

**Table 2**
Kinetic resolution of 1,2-diphenylethane-1,2-diol by the Cu@1-Ph-PMO and in **1** and **2** in homogeneous phase (Scheme 3).[a]

| | Run | %mol[b] | | %yield[c] | %ee[d] | *S*[e] | TON[f] |
|---|---|---|---|---|---|---|---|
| | | Cu | Ligand | | | | |
| Without catalyst | | | | 21 | 0 | | |
| **1** + [Cu(OTf)$_2$] | | 1.0 | 1.0 | 46 | 84 | 27 | 46 |
| **2** + [Cu(OTf)$_2$] | | 1.0 | 1.0 | 47 | >99 | >581 | 45 |
| Cu@1-Ph-PMO | 1st | 1.0 | 6.0 | 45 | 94 | 76 | 46 |
| | 2nd | 0.9 | 5.6 | 44 | >99 | 460 | 47 |
| | 3rd | 0.9 | 5.4 | 46 | 98 | 264 | 53 |
| | 4th | 0.9 | 5.4 | 46 | 97 | 172 | 52 |
| | 5th | 0.7 | 4.5 | 43 | 91 | 43 | 58 |
| graf_Cu-1@Ph-PMO | 1st | 0.8 | 0.8 | 38 | 66 | 7 | 50 |
| | 2nd | 0.8 | 0.7 | 37 | 64 | 7 | 50 |

[a] Reactions performed for 24 h at 0 °C using 0.48 mmol (*R*,*R*)-**3**, 0.48 mmol (*S*,*S*)-**3**, 1.00 mmol DIPEA, 1.0% mol based on Cu and 0.50 mmol of benzoyl chloride in 5.0 ml of $CH_2Cl_2$.

[b] Percentage of copper and ligand **1** in the catalyst in relation to **3** (see Table 1); for the recycling experiments corrected for the loss of heterogeneous catalyst weight.

[c] Isolated yield of **4** (Scheme 3).

[d] Enantiomeric excess of **4**, determined by HPLC.

[e] Selectivity ($S$) = ln[1 − yield (1 + ee)]/ln[1 − yield (1 − ee)].

[f] TON = moles of isolated **4**/moles of Cu.

## 4. Conclusions

A novel mesoporous chiral Cu(II) bis(oxazoline) phenylene-silica with narrow distribution of pores is proved to be easily prepared by a co-condensation methodology. Upon coordination of Cu(II) triflate complex, this material acts as a highly efficient and reusable catalyst on the kinetic resolution of 1,2-diphenylethane-1,2-diol. Moreover, the material shows improved catalytic activity and superior enantioselectivity comparing to the homogeneous counterpart, while being recyclable at least up to four consecutive cycles. The preparation method seems to be extremely important on the definition of the final properties of the heterogeneous catalysts. The co-condensation of bis-silylated precursors showed to be efficient on avoiding the leaching of the metal complex.

## Acknowledgments

Authors are grateful to the Fundação para a Ciência e a Tecnologia (FCT), Fundo Europeu de Desenvolvimento Regional (FEDER), QREN-COMPETE, the European Union, and the Associate Laboratory CICECO for funding the Projects PTDC/QUI-QUI/64770/2006, FCOMP-01-0124-FEDER-015644 (PTDC/QUI-QUI/113678/2009), FCOMP-01-0124-FEDER-037271 (PEst-C/CTM/LA0011/2013). ARS thanks FCT, FSE and POPH for the contract under the program *Ciência 2008*. ARS and PF acknowledge IF/01300/2012 and IF/00327/2013, respectively. MAOL thanks the PhD grant SFRH/BD/80883/2011. The research leading to these results has received funding from the European Union Seventh Framework Programme under Grant Agreement 312483 – ESTEEM2 (Integrated Infrastructure Initiative–I3).

## Appendix A. Supplementary data

Supplementary data associated with this article can be found, in the online version, at http://dx.doi.org/10.1016/j.jcat.2014.09.017.

## References

[1] G. Desimoni, G. Faita, K.A. Jorgensen, Chem. Rev. 111 (2011) 284.
[2] D. Rechavi, M. Lemaire, Chem. Rev. 102 (2002) 3467.
[3] A.F. Trindade, P.M.P. Gois, C.A.M. Afonso, Chem. Rev. 109 (2009) 418.
[4] J.M. Fraile, J.I. Garcia, J.A. Mayoral, Chem. Rev. 109 (2009) 360.
[5] J.M. Fraile, J.I. Garcia, C.I. Herrerias, J.A. Mayoral, E. Pires, Chem. Soc. Rev. 38 (2009) 695.
[6] D. Rechavi, M. Lemaire, Org. Lett. 3 (2001) 2493.
[7] R. Annunziata, M. Benaglia, M. Cinquini, F. Cozzi, M. Pitillo, J. Org. Chem. 66 (2001) 3160.
[8] M.I. Burguete, J.M. Fraile, J.I. Garcia, E. Garcia-Verdugo, C.I. Herrerias, S.V. Luis, J.A. Mayoral, J. Org. Chem. 66 (2001) 8893.
[9] S.S. Lee, S. Hadinoto, J.Y. Ying, Adv. Synth. Catal. 348 (2006) 1248.
[10] S.S. Lee, J.Y. Ying, J. Mol. Catal. A-Chem. 256 (2006) 219.

[11] A.R. Silva, H. Albuquerque, S. Borges, R. Siegel, L. Mafra, A.P. Carvalho, J. Pires, Micropor. Mesopor. Mater. 158 (2012) 26.
[12] A.R. Silva, V. Guimarães, A.P. Carvalho, J. Pires, Catal. Sci. Technol. 3 (2013) 659.
[13] A.R. Silva, L. Carneiro, A.P. Carvalho, J. Pires, Catal. Sci. Technol. 3 (2013) 2415.
[14] J. Lim, S.N. Riduan, S.S. Lee, J.Y. Ying, Adv. Synth. Catal. 350 (2008) 1295.
[15] P. Borah, X. Ma, K.T. Nguyen, Y.L. Zhao, Ang. Chem.-Int. Ed. 51 (2012) 7756.
[16] K.M.T. Seki, C.M. Crudden, Chem. Commun. (2012) 6369.
[17] M. Waki, N. Mizoshita, T. Tani, S. Inagaki, Ang. Chem.-Int. Ed. 50 (2011) 11667.
[18] X. Liu, P.Y. Wang, Y. Yang, P. Wang, Q.H. Yang, Chem. Asian J. 5 (2010) 1232.
[19] C. Baleizao, B. Gigante, D. Das, M. Alvaro, H. Garcia, A. Corma, J. Catal. 223 (2004) 106.
[20] B. Gigante, C. Baleizão, D. Das, M. Alvaro, H. Garcia, A. Corma, Chem. Commun. (2003) 1860.
[21] N. Mizoshita, T. Tani, S. Inagaki, Chem. Soc. Rev. 40 (2011) 789.
[22] P. Van Der Voort, D. Esquivel, E. De Canck, F. Goethals, I. Van Driessche, F.J. Romero-Salguero, Chem. Soc. Rev. 42 (2013) 3913.
[23] A.R. Silva, Curr. Org. Chem. 18 (2014) 1225.
[24] R.J. Clarke, I.J. Shannon, Chem. Commun. (2001) 1936.
[25] R.J.P. Corriu, J.J.E. Moreau, P. Thepot, M. W. Chi Man 4 (1992) 1217.
[26] S. Inagaki, S. Guan, T. Ohsuna, O. Terasaki, Nature 416 (2002) 304.
[27] M. Kruk, V. Antochshuk, M. Jaroniec, A. Sayari, J. Phys. Chem. B 103 (1999) 10670.
[28] S.J. Gregg, K.S.W. Sing, Adsorption, Surface Area and Porosity, second ed., Academic Press, London, 1982.
[29] Y. Matsumura, T. Maki, S. Murakami, O. Onomura, J. Am. Chem. Soc. 125 (2003) 2052.
[30] Q. Yang, M.P. Kapoor, S. Inagaki, J. Am. Chem. Soc. 124 (2002) 9694.
[31] M.E. Owen, E. Carter, G.J. Hutchings, B.D. Ward, D.M. Murphy, Dalton Trans. 41 (2012) 11085.
[32] J.M. Fraile, J.I. Garcia, C.I. Herrerias, J.A. Mayoral, Chem. Commun. (2005) 4669.
[33] A. Gissibl, M.G. Finn, O. Reiser, Org. Lett. 7 (2005) 2325.
[34] A. Schatz, M. Hager, O. Reiser, Adv. Funct. Mater. 19 (2009) 2109.
[35] A. Schatz, R.N. Grass, Q. Kainz, W.J. Stark, O. Reiser, Chem. Mater. 22 (2010) 305.
[36] M.P. Conley, C. Copeŕet, C. Thieuleux, ACS Catal. 4 (2014) 1458.